QUARKS: Brazilian Electronic Journal of Physics, Chemistry and Material Science
journal homepage: https://periodicos.ufjf.br/index.php/quarks
e-ISSN: 2674-9688

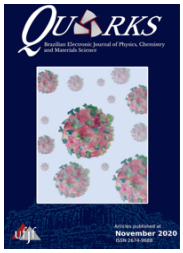

Thyroxine: A Theoretical Study of the Vibrational and Electronic Properties

Ricardo V. K. Rizzon, Zélia M. Da Costa Ludwig, Lucas Modesto-Costa, Valdemir Ludwig*

Departamento de Física, Universidade Federal de Juiz de Fora, CP 36036-330, Juiz de Fora, MG, Brazil.

Article history: Received: August 2020; Revised: September 2020; Accepted: October 2020. Available online: November 2020.
https://doi.org/10.34019/2674-9688.2020.v3.30941

Abstract

Through this work, we systematically studied the structural, vibrational and electronic properties of the fundamental state of the isolated thyroxine(3,5,3',5-tetraiodothyronine). The minimum energy structures and properties were obtained using the Density Functional Theory (DFT). Our simulation results were compared with experimental results, including infra-red and Raman spectroscopy with an emphasis on the properties of iodine atoms. The UV-vis spectrum calculated in this work is the first result of this model for the thyroxine molecule.

Keywords: Thyroxine, Density Functional Theory, Raman.

1. Introduction

Disorders in thyroid functions cause an imbalance in the production of thyroid hormones, leading to the occurrence of metabolic dysfunctions throughout the body, which are mainly diagnosed by clinical symptoms. According to the Brazilian Society of Endocrinology and Metabology (SBEM), approximately 300 million people worldwide suffer from thyroid dysfunction, although more than half are unaware of this condition [1]. In Brazil, about 15% of the population suffers from thyroid problems, according to data released by the Brazilian Institute of Geography and Statistics (IBGE), with the elderly and women being the most susceptible to dysfunctions [2]. When it is overactive and produces excess hormones, it causes hyperthyroidism. The condition can cause tachycardia, nervousness, weight loss, excessive sweating and irregular menstruation. Hypothyroidism is the opposite extreme. Insufficient production of hormones can cause fatigue, weight gain, cold intolerance, dry skin, hair loss and increased menstrual flow. When these cases are not diagnosed and identified, thyroid disease can progress to more serious conditions [3]. The biosensor appears as a promising alternative, as it has advantages and works as a useful tool in the diagnosis of various diseases, as already known commercially available for monitoring and diagnosis of diabetes. Thus, a simple, fast and low-cost diagnosis is based on the use of spectroscopic techniques for the detection of biomolecules and biosensors.

Several researchers worked on different important biomolecules, in particular, the characterization of the vibrational modes of thyroxine was explored by Álvarez et al [4] using Raman spectroscopy. More recently, a theoretical/experimental [5] with the Fourier-transform infrared spectroscopy (FT-IR) and Raman techniques have been used to record the

*Corresponding author. E-mail: ludwig.valdemir@gmail.com

spectra of Thyroxine molecule and correlated with experimental data. However, there has been limited investigation of the thyroid system and they still remain a bit of mystery in the functionality of this molecule. It is necessary to have a detailed UV-vis spectroscopic study of this biomolecule.

In this study we investigated the structure, vibrational and electronic properties of the thyroxine molecule, also named T_4 or L-thyroxine, IUPAC name 3,5,3′,5′-tetraiodothyronine, making a systematic analysis of the FT-IR, Raman and UV-vis spectra. The structure of the molecule is obtained by minimizing the energy using two different Density Functional Theory (DFT) functionals, one hybrid and another one non-hybrid. Thus, we present in detail the equilibrium structure and the vibrational properties. After obtaining these minimum geometries the electronic properties were explored by analyzing the UV-vis spectrum and the electronic transitions. MPPST and compared with results reported in the existing literature.

In Section 2 basic details of both theoretical methods are shown; in Section 3 results are presented and discussed and finally, in Section 4 we present the conclusions.

2. Material and Methods

All of the DFT based calculations reported for the thyroxine were carried out using the Orca software [6]. A preliminary geometry optimization was performed by energy minimization using molecular mechanics with MMFF94 force field and steepest descent algorithm. These geometric parameters were used as input for the main optimizations performed with the hybrid B3LYP [7, 8] and non-hybrid BP86 [8,9] generalized gradient approximation (GGA) functionals and the split valence polarization (SVP) double-zeta basis set [10] for C, O and H atoms. For the Iodine atom, the effective core potential (ECP-28) was used to replace the 28 core electrons [11] and the remaining 25 electrons were treated explicitly. For the remaining 25 electrons, the triple-zeta polarization basis set function was used from the Ahalrichs Def2 basis set family [10]. The harmonic vibrational frequencies have been checked for the optimized structures to confirm that the true energy minimum has been found. Both infra-red and Raman harmonic vibrational modes were calculated and uniformly scaled by a factor of 0.98 and 0.96 [12] respectively for B3LYP and BP86 functionals. The simulated spectra were calculated to the models followed by a 10 cm^{-1} half-width convolution. The same analyses have done in our previous work [13].

The time dependent (TD-DFT) approaches were used to predict 30 vertical excitations since this is typically sufficient for the interpretation of the most intense peak observed in the UV-vis spectra. To accelerate the electronic absorption calculation, the RIJCOSX [14] was used with the inclusion of auxiliary basis sets [15]. In each case, the output files along with detailed information about energies, oscillator strengths, wave functions of corresponding excitations, and absorption spectra via transition electric dipole moments. The UV-vis spectrum was simulated with the convolution of the individual vertical excitations and the oscillator strengths using 10nm half-width. The oscillator strength is obtained by the transition electric dipole moments.

3. Results and Discussion

3.1 Geometry Optimization

To obtain the calculated vibrational spectra, the conformational structures were optimized by employing DFT calculations and the

minimum energy conformations were presented in Figure 1. The structural composition of the thyroxine molecule in the ground state energy level is linear with the two rings rotated by 90 degrees each other. The input geometrical parameters used were obtained from the energy minimization carried out by molecular mechanics and the optimized parameters obtained by B3LYP and BP86 were presented in table 1. The X-ray diffraction, XRD, were presented for the internal bond distances [16]. The first 10 lines, in the left side of the table were related to the benzene rings in the molecule. Our calculated values show a variation from 1,396 to 1,416 Å for the two functionals used. The BP86 functional provides a slightly higher value compared to the B3LYP functional. The experimental values of x-ray diffraction were slightly different with a order of 0.04 Å for most bonds except for the C12-C13 were e a difference of more than 0.1 Å was obtained. Higher values were obtained for the C-C bonds associated with carbon chains attached to the C5 of ring and listed in the next 3 parameters of the table. The bonds between the carbons and iodine atoms have bonds greater than 2 Å and the calculated values are close to the experimental values. Compared to the experimental values we found that the distance of the C1-I19 bond is larger by approximately 0.044 Å, in agreement with the previous calculated value for this bond by Borah and Devi [5]. Bonding distance between C-O show a small variation and with lower values for connections C28-O33 and C28-O35. In general, the structures obtained are in comparison with the previous experimental and theoretical results.

3.2 Vibrational Properties

The thyroxine molecule has 35 atoms and therefore results in 99 vibrational modes, all active in both the IR and Raman spectra. The main absorption bands for the thyroxine molecule obtained by the B3LYP and BP86 functionals are in accordance. As we can see that with the non-hybrid functional BP86 we can obtain results for IR and Raman spectra very similar to those of a functional hybrid B3LYP with 50% less in computational time. The calculated FT-IR and Raman spectra of thyroxine were compared with the experimental spectrum extracted from the experimental one reported by Borah and Devi [5] for thyroxine monomer, in figure 2. Our analyses start at the low frequencies were the C-I stretching mode can be observed.

Thyroxine monomer has four Iodine atoms in the two benzene rings. In the literature, the C-I stretching vibrations are found to be in between 300 - 550 cm^{-1}. In the experimental IR spectrum, no peaks with great intensity were found. On the other hand, the Raman spectrum presents intense peaks in the region of low frequencies. Our results for the calculated vibrational modes for calculated for the C-I stretch showed little intensity in both in the region of 300-550cm^{-1}. These values were in accordance with previous calculated vibrational frequencies calculated by Borah and Devi [5] for similar thyroxine molecule.

Table 1: Calculated bond length of thyroxine molecule. The X-ray diffraction (XRD) values were obtained from the work of Camerman [16].

Bond	B3LYP	BP86	XRD	Ref.[5]
C13-C12	1.406	1.407	1.26	1.42
C12-C11	1.398	1.400	1.47	1.40
C11-C10	1.394	1.394	1.39	1.40
C10-C9	1.398	1.399	1.42	1.40
C1-C3	1.405	1.406	1.38	1.41
C3-C6	1.408	1.408	1.38	1.41
C6-C4	1.396	1.397	1.49	1.40
C4-C5	1.404	1.404	1.35	1.41
C5-C2	1.401	1.401	1.49	1.41
C2-C1	1.398	1.399	1.45	1.41
C5-C24	1.514	1.514	1.52	1.52
C24-C25	1.556	1.556	1.56	1.56
C25-C28	1.544	1.545	1.54	1.53
C12-I23	2.113	2.126	2.15	2.15
C1-I19	2.103	2.114	2.06	2.13
C6-I18	2.104	2.114	2.11	2.13
C13-O21	1.346	1.348	1.34	1.39
C10-O17	1.380	1.380	1.41	1.41
C3-O17	1.367	1.366	1.41	1.40
C28-O33	1.351	1.354	1.28	1.39
C28-O35	1.200	1.200	1.24	1.24
C25-N29	1.449	1.450	1.52	1.47

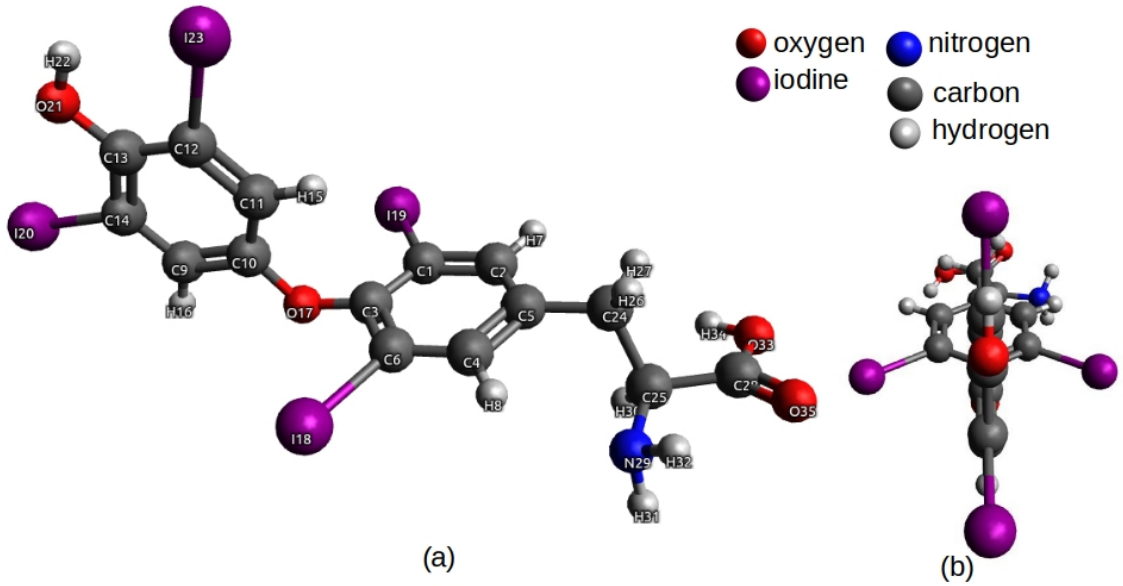

Figure 1: Three-dimensional structure of the thyroxine molecule in two views: (a) lateral view and (b) front view. The colors of the bolls were listed in the upper right corner.

The deformation vibrational modes were located with medium intensities in the region of 700-900cm^{-1} and also in intense lines in the region of 1220-1320cm^{-1} in the Raman spectroscopy. These vibrational modes can be related to medium intense lines in the experimental Raman spectra at 900cm^{-1} and 1300cm^{-1}. In the IR spectrum, small intense were in the region of 800-1000cm^{-1} and 1200cm^{-1} in coincidence with our convoluted spectra for both B3LYP and BP86 functionals.

Intense lines in the IR were calculated with a peak at 1409 cm^{-1} for the vibrational stretches C-C and C=C and a medium intense peak located at 1808 cm^{-1} for the vibrational mode C=O. The experimental lines for the C=O were observed in smaller frequencies at 1700 cm^{-1} with maximum intensities.

Three different groups were clearly identified at the high frequency region, the C-H, N-H and O-H strengths were calculated at 2921, 3074 and 3400-3600cm^{-1} for the IR spectrum with low intensities. In the experimental spectra the same vibrational modes were obtained at 3065 3261 and 3515 cm^{-1}. Large intensities were observed in the Raman spectra with in the three different regions and our calculated values of were 100-200cm^{-1} higher compared to the experimental values.

The molecular structure of minimum calculated energy the two functionals were employed to the electronic excitations calculation and obtain transition energies of the thyroxine molecule in the ultra-violet visible region. The results will be presented in the next section.

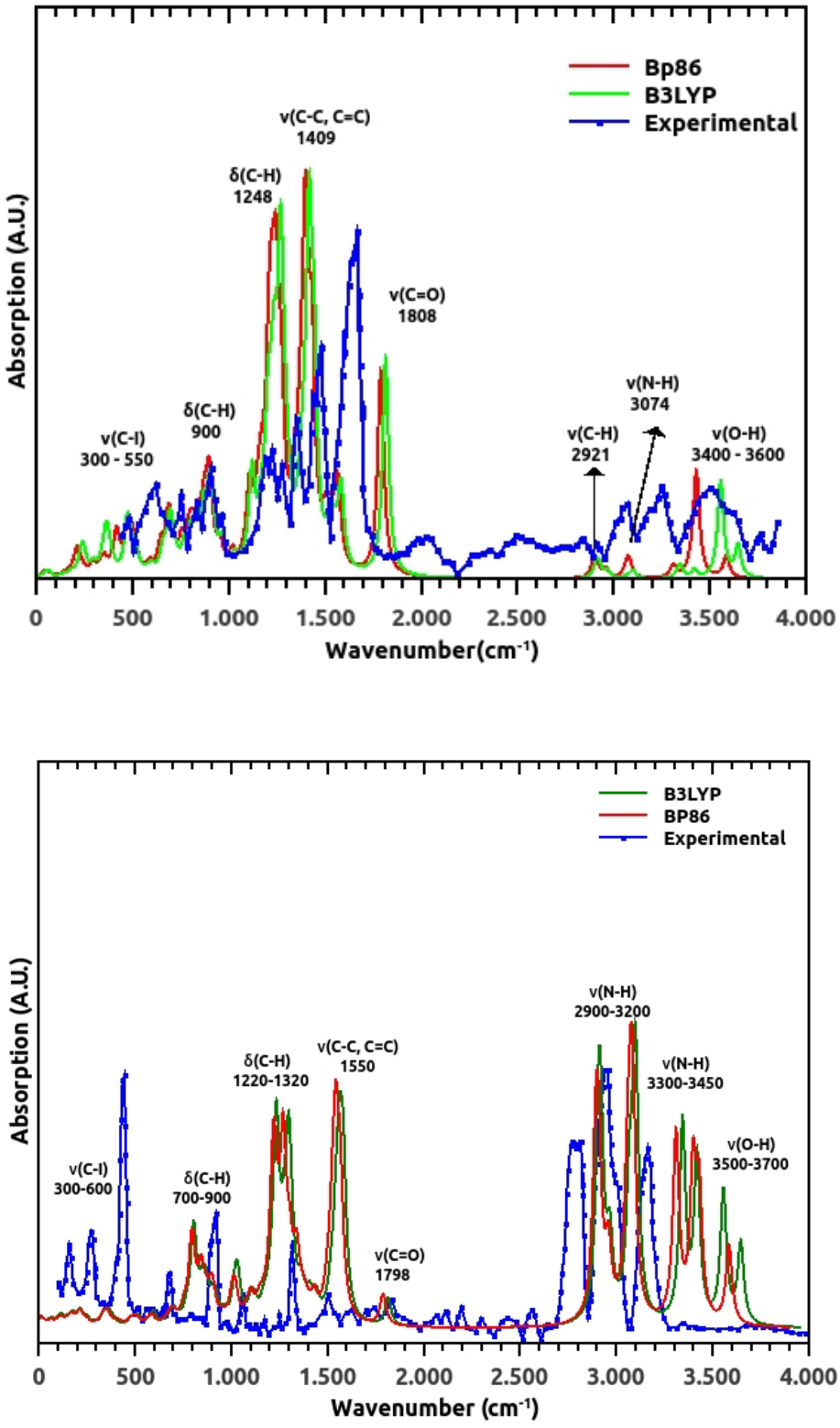

Figure 2: Experimental and convoluted FT-IR (top) and Raman (bottom) spectra of thyroxine molecule in the range of 0-4000 cm^{-1}. The main peaks of the spectra are associated with the vibration modes found in the molecule.

3.3 UV-vis spectra

The UV-vis spectrum measured using absorption spectroscopy in distilled water and a temperature of 300 K [17] showed in Figure 3. In the region of 200 to 400 nm, the spectrum shows 2 main broad peaks at 238 and 280nm. The calculated spectrum for each DFT functional is formed by the convolution of gaussians with 10 nm of the half-width of individual excitations. The spectra for the B3LYP and BP86 models show a low energy excitation, around 370 nm. In addition, the most intense band arise in 305 nm, before the experimental and B3LYP results. The number of roots used to produce the spectrum curves were carefully tested in order to obtain curves that were in better agreement with the experimental curves. The functional B3LYP is the one that best matches the experimental curve. The curve obtained by BP86 is shifted to longer wavelengths. The functional B3LYP produces results very close to those of the experimental spectrum, with two bands with the maximums located in 239 and 270 nm. In addition, the shape of the convoluted spectrum corresponds to the experimental spectrum. The first experimental band is wide, and both theoretical models show the same band with a shoulder in higher wavelengths. This discrepancy in the theoretical results reveals the sensitivity of some functionals in describing the excitations at the electronic levels. We did not find in the literature theoretical results with similar methods for this molecule. In a recent work, several popular exchange-correlation functionals were used for the prediction of UV-visible (vis) - near infrared (NIR) spectra of phthalocyanines [18] and the conclusion that these authors reached was that hybrid functionals are necessary to better describe the UV-visible spectrum.

We also analyzed the character of Kohn-Sham molecular orbitals involved in the most intense transitions, Figure 4. For the peak at 237 nm, the most intense transition (29^{th}) is formed by different characters where the most dominant (32 %) is characterized by HOMO-5 to LUMO. This transition is related to transitions involving the chain and carbonyl group of one ring and the iodine atoms of the other ring, as can be seen at the second row of Figure 4. Therefore, in this transition, we identified a charge-transfer transition. For the peak at 270 nm, the most intense transition is dominated by HOMO to LUMO+4 (78 %). This transition involving orbitals from the left side ring, between the iodine atoms to the internal ring.

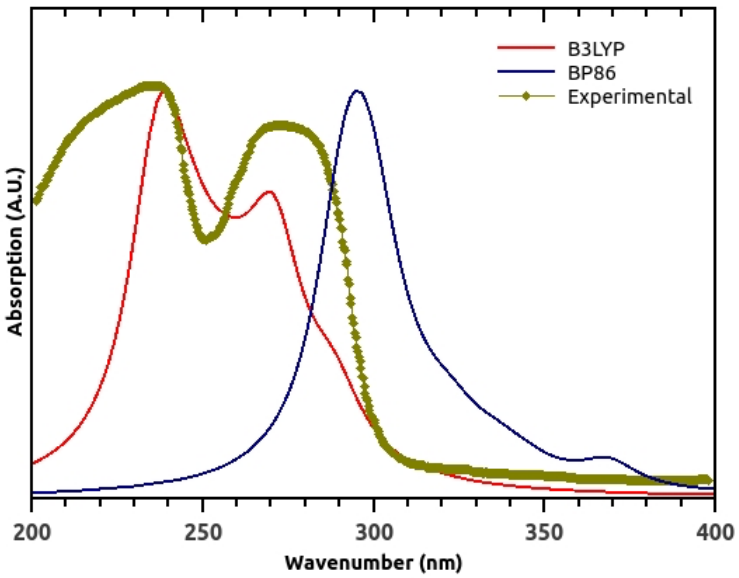

Figure 3: Experimental and convoluted UV-vis spectra in the range of 200-400nm (25000-50000cm^{-1}).

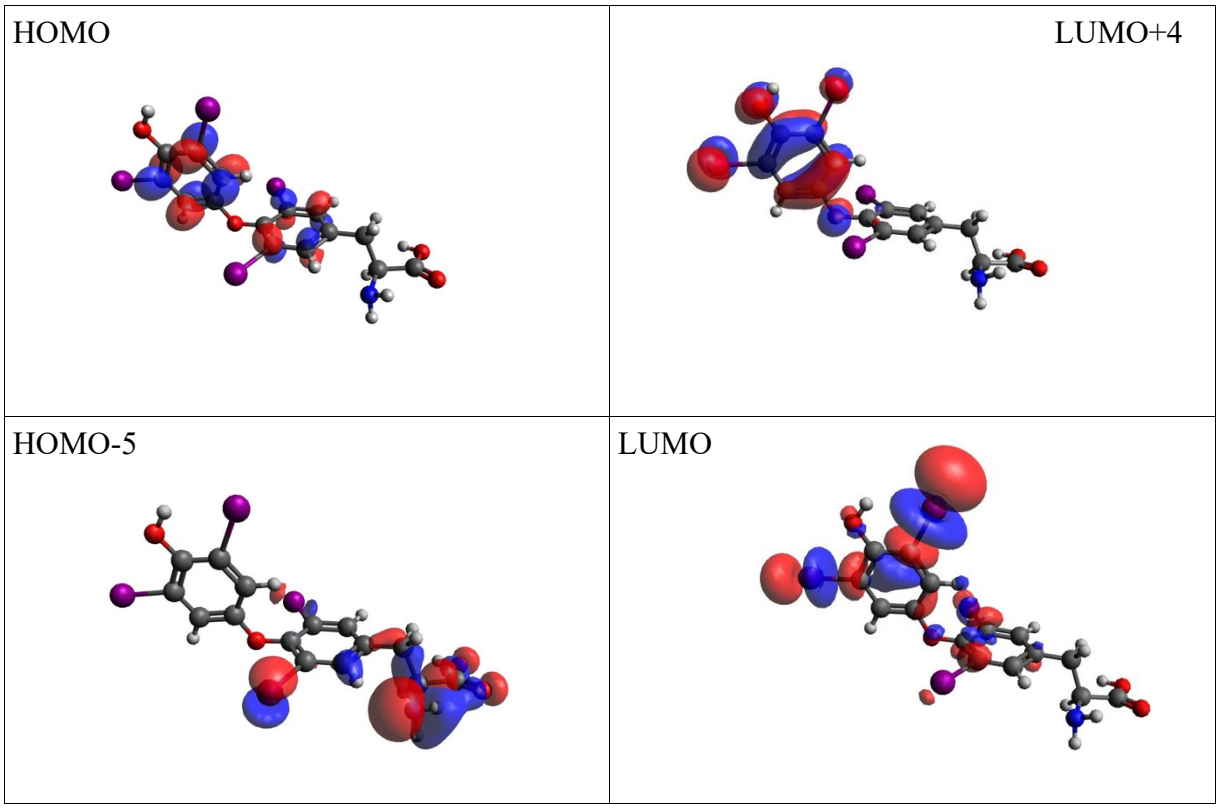

Figure 4: Kohn-Sham molecular orbitals of the most intense transitions calculated with B3LYP functional. At the top row, the character orbitals involved in the most intense transition of the peak at 271 nm. At the bottom row, the character orbitals involved in the most intense transition of the peak at 237 nm.

4. Conclusions

In this study, we present the results of vibrational and electronic properties for a thyroxine molecule using the B3LYP and BP86 DFT functionals. The minimum energies structure calculated by both methods are close and in accordance with the previous experimental values. The vibrational modes and the convoluted spectra for both IR and Raman techniques results in similar results and indicates that the BP86 function was successful in describing the minimal energy structure for thyroxine. Our results for electronic excitations and the UV-vis spectrum indicated that the B3LYP functional presents significantly better results and the two peaks observed in the experimental results were identified. These results for the UV-vis spectrum are the first results calculated for the thyroxine molecule under the DFT model and the analysis of the transitions at the electronic levels, in particular in the charge transfer states, is indicative that the knowledge of the electronic properties of the system can improve the development of sensors for the diagnosis of thyroid hormone on platforms built with modified materials such as graphene.

Acknowledgments

The authors thanks to Brazilian funds CNPq, Fapemig and the high-performance computer facilities of the LNCC and the National Laboratory for Scientific Computing (LNCC/MCTI, Brazil).

References and Notes

[1] Brazilian Society of Endocrinology and Metabology. International Thyroid Week. 2011 http://www.tireoide.org.br/semana-internacional-da-tireoide-2020/ Accessed on: June 1, 2020.

[2]https://www.spdm.org.br/saude/noticias/item/1755-tireoide-a-maestrina-das-celulas Accessed on: June 1, 2020.

[3] M. S. Segatto, Masters dissertation: Development of the functionalized graphite platform with poly (4-hydroxyphenylacetic acid) on reduced graphene oxide - gold nanoparticles for the detection of the hormone triiodothyronine, Universidade Federal de Uberlândia.

[4] R. M. S. Alvarez, R. N. Faris and P. Hildebrandt, Comparative vibrational analysis of thyronine hormones using infrared and Raman spectroscopy and density functional theory calculations J. Raman Spectrosc. 35 (2004) 947-955.

[5] M. M. Borah and T. G. Devi, Vibrational studies of Thyroxine hormone: Comparative study with quantum chemical calculations Journal of Molecular Structure 1148 (2017) 293-313.

[6] F. Neese, The ORCA program system. Wiley Interdiscip Rev Comput Mol Sci 2012, 2:73–78.

[7] C. Lee, W. Yang and R. G. Parr, Development of the Colle-Salvetti correlation-energy formula into a functional of the electron density, Phys. Rev. B, **37** (1988) 785-89.

[8] A. D. Becke, Density-functional exchange-energy approximation with correct asymptotic-behavior, Phys. Rev. A, 1988 38 3098-100.

[9] J. P. Perdew, Density-functional approximation for the correlation energy of the inhomogeneous electron gas, Phys. Rev. B, 1986 33 8822-24.

[10] F. Weigend, and R. Ahlrichs, Balanced basis sets of split valence, triple zeta valence and quadruple zeta valence quality for H to Rn: design and assessment of accuracy, Phys. Chem. Chem. Phys. 2005 7 3297–3305.

[11] K. A. Peterson, Systematically convergent basis sets with relativistic pseudopotentials. II. Small-core pseudopotentials and correlation consistent basis sets for the post-d group 16-18elements J. Chem. Phys., 2003 119, 11113-11123.

[12] P. Sinha, S. E. Boesch, C. Gu, R. A. Wheeler, A. K. Wilson, Harmonic vibrational frequencies: scaling factors for HF, B 32 methods in combination with correlation consistent basis sets, J. Phys. Chem. A 2004,108, 9213–9217.

[13] V. Ludwig, Z. M. da Costa Ludwig, M. M. Rodrigues, V. Anjos, C. B. Costa, D. R. Sant'Anna das Dores, V. R. Silva, and F. Soares, Analysis by

Raman and infrared spectroscopy combined with theoretical studies on the identification of plasticizer in PVC films. Vibrational Spectroscopy 2018 98 134–138.

[14] F. Neese, F. Wennmohs, A. Hansen, U. Becker, Efficient, approximate and parallel Hartree–Fock and hybrid DFT calculations. A 'chain-of-spheres' algorithm for the Hartree–Fock exchange Chem. Phys., 2009 356, 98-109.

[15] F. Weigend, Accurate Coulomb-fitting basis sets for H to Rn, Phys. Chem. Chem. Phys. 2006,8 1057-1065.

[16] A. Camerman and N. Camerman, Thyroid hormone stereochemistry. I. The molecular structures of 3,5,3'-triiodo-L-thyronine (T_3) and L-thyroxine (T_4), Acta Cryst. 30B (1974) 1832-1840.

[17] F. F. Al-Kazzaz, and D. R. Dhalia, Biophysical Study on Thyroxine (T4) and its crude recepters in thyroid tissues, Journal of Chemical and Pharmaceutical Research, 2012, 4(1):673-685.

[18] G. Alexander, A. G. Martynov, J. Mack, A. K. May, T. Nyokong, Y. G. Gorbunova and A. Y. Tsivadze, Methodological Survey of Simplified TD-DFT Methods for Fast and Accurate Interpretation of UV–Vis–NIR Spectra of Phthalocyanines, ACS Omega 2019, 4, 7265−7284.